INORGANIC CHEMISTRY FRONTIERS

RESEARCH ARTICLE

View Article Online
View Journal

Cite this: DOI: 10.1039/d4qi03227f

Published on 03 June 2025. Downloaded by Yunnan University on 7/31/2025 4:04:30 PM.

Structural anchoring of highly reactive CBH⁻ for high-performance hypergolic coordination polymers with excellent thermal stability†

Qin Wang,‡[a] Meng Cui,‡[b] Pin-Hao Wei,[a] Long-Chuan Li,[a] Ning-Ning Zhang,[c] Fei Tan,[a] Fa-Kun Zheng,*[b] Jian-Gang Xu*[a,b] and Guo-Cong Guo[b]

The energetic BH_3CN^- anions (named CBH^-) have attracted significant interest in hypergolic materials due to their high energy density and strong reducibility. However, most CBH^--based hypergolic materials typically suffer from low stabilities. Structurally stabilizing the CBH^- anion to design materials with stable and excellent hypergolic performance continues to present significant challenges. To resolve these issues, we herein propose the first strategy to structurally anchor the high-activity CBH^- anion within the coordination polymer (CPs) platform to obtain three hypergolic and structurally similar CPs $[M(CBH)_2(BIM)_2]_n$ (M = Cd **1**, Mn **2**, Zn **3**; BIM = bis(1-imidazolyl) methane). Compounds **1–3** exhibit remarkable stability, outstanding high volumetric energy densities (E_v), and short ignition delay (ID) times. The E_v values of **1–3** are all greater than 36 kJ cm^{-3}, which are significantly higher than that of commercial unsymmetrical dimethylhydrazine (UDMH) with E_v = 25.60 kJ cm^{-3}. In particular, the Mn-based **2** demonstrates the highest thermal stability (T_{dec} = 317 °C) among all CBH-based hypergolic materials, attributed to the unique coordination polymerization method for CBH^- anions. Among the three compounds, the Cd-based **1** exhibits the shortest ID time (12 ms) when ignited with white fuming nitric acid (WFNA), which might be ascribed to the highest molecular polarity and smallest band gap of **1** by theoretical calculations. This study presents a precise structural design strategy for the rational design of highly active and stable hypergolic fuels for propellant applications.

Received 16th December 2024,
Accepted 4th February 2025

DOI: 10.1039/d4qi03227f

rsc.li/frontiers-inorganic

Introduction

Hypergolic materials, which ignite spontaneously upon contact with an external oxidizer, are critically significant as fuels and propellants in the military and aerospace fields.[1–4] The most prevalent hypergolic fuels in bipropellant systems are derived from hydrazine and its derivatives, such as monomethyl hydrazine (MMH) and unsymmetrical dimethylhydrazine (UDMH), due to their high specific impulse (I_{sp}) and short ignition delay (ID) time when combined with oxidizers like white fuming nitric acid (WFNA). However, these hypergolic materials present several challenges, including environmental pollution and high storage and transportation costs due to their corrosiveness, toxicity, and volatility.[3,5–8] Therefore, the next generation of hypergolic materials should possess the following properties: (a) high specific impulses; (b) high energy densities; (c) short ignition delay times (ID ≤ 50 ms); (d) good stabilities to ensure convenient and safe transport and storage; (e) stable combustion characteristics; (f) inexpensive and safe synthesis; and (g) environmentally acceptable manner.[9–12]

To develop high-performance hypergolic fuels to satisfy the aforementioned requirements, several research systems have been developed and mainly classified into energetic ionic liquids and energetic metal complexes. In 2008, dicyanamide-based energetic ionic liquids (ILs) were first reported as hypergolic materials.[13] Subsequently, a variety of hypergolic ILs with short ID times and low vapor pressure have been reported successively,[14,15] such as 1-ethyl-1,1-dimethylhydrazinium cyanoborohydride (EDCBH) and 1-butyl-1,1-dimethylhydrazinium cyanoborohydride (BDCBH).[16] Unfortunately, the low energy

---

[a] College of Material Engineering, Fujian Agriculture and Forestry University, Fuzhou 350108, China. E-mail: jgxu@fafu.edu.cn

[b] State Key Laboratory of Structural Chemistry, Fujian Institute of Research on the Structure of Matter, Chinese Academy of Sciences, Fuzhou, Fujian 350002, P. R. China. E-mail: zfk@fjirsm.ac.cn

[c] School of Chemistry and Chemical Engineering, Liaocheng University, Liaocheng, Shandong 252000, P. R. China

† Electronic supplementary information (ESI) available: X-ray crystallographic data for **1–3**, heat of combustion, sensitivity tests, specific impulse, thrust coefficient and FT-IR spectra. CCDC (**1**),[51] 2329590 for (**2**) and 2329589 for (**3**). For ESI and crystallographic data in CIF or other electronic format see DOI: **https://doi.org/10.1039/d4qi03227f**

‡ These authors contributed equally to this work.

Published on 03 June 2025. Downloaded by Yunnan University on 7/31/2025 4:04:30 PM.

density, insufficient combustion performance, and complex preparation process of these ILs significantly limit their broad application.[17–19]

Hypergolic coordination polymers (HCPs) offer a versatile molecular design platform, allowing precise tailoring of structures and properties through variations in metal centers and energetic ligands. HCPs have demonstrated advantageous energetic properties, such as high energy densities, excellent thermostability, and remarkable mechanical strength due to their reinforced structures.[20–24] In 2019, Rogers and co-workers first revealed zeolitic imidazolate frameworks (ZIFs) with excellent hypergolic response and thermal degradation above 200 °C (Scheme 1a), such as $Zn(AIM)_2$ and $Zn(VIM)_2$ (HVIM = vinyl imidazolate, HAIM = acetylene imidazolate); however, their energy densities are not outstanding enough (volumetric energy densities (E_v) = 19.30 and 18.90 kJ cm^{-3}).[25] To enhance the energy densities of hypergolic coordination compounds (HCCs), Li and co-workers utilized the high-energy, strongly reductive cyanoborohydride (CBH) anions and monodentate imidazole ligands to prepare a series of compounds, such as Cu-MIm-CBH (MIm = 1-methylimidazole) and Cu-EIm-CBH (EIm = 1-ethylimidazole), with E_v values ranging from 33.47 to 36.67 kJ cm^{-3}.[26] Regrettably, the thermal stabilities of these hypergolic materials are all below 200 °C due to isolated structures (Scheme 1a). Subsequently, many scholars have utilized different energetic anions and cations to prepare HCCs, such as $[Cu_6Ag_8(C_4B_{10}H_{11})_{12}Cl]\cdot NO_3$ (CBA-CuAg) ($C_4B_{10}H_{11}$ = *o*-carborane-alkynyl),[4] $[M(DCA)_2(1\text{-}VIM)_2]_n$ (1-VIM = 1-vinylimidazole, DCA = dicyandiamide),[9] $[Cu_4Br_6(PMIM)_2]_n$ ([PMIM] = 1-propargyl-3-methylimidazolium),[27] $Mn(AIM)_3(NO_3)_2$, $Cu(AIM)_4Cl_2$, (AIM = 1-allylimidazole),[28] and $[NH_4]_2[Cu(BTA)_2]_n\cdot H_2O$ (named CuBTA, H_2BTA = bis(5-tetrazolyl)amine).[29] These HCCs demonstrate stable hypergolic performance and short ID times, highlighting their potential as viable alternatives to traditional hypergolic fuels. Despite these advancements, currently reported HCCs are primarily limited to simple assemblies of energetic components. Many HCCs exhibit low thermal stability with isolated structures and low energy densities with non-energetic solvent molecules and halogen components. These approaches still face challenges in achieving HCCs with superior comprehensive performance. Therefore, achieving HCCs with high energy densities, short ID times and good stabilities through precise structural design remains in its early stages.

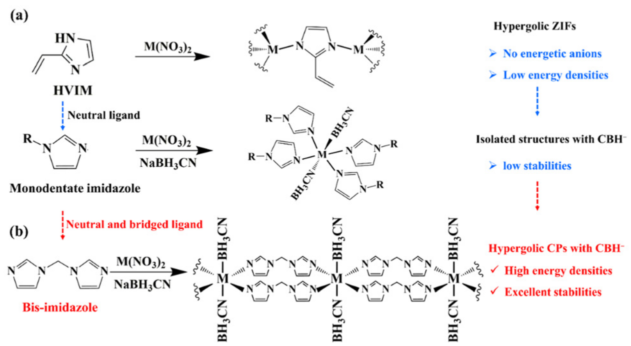

Scheme 1 Design strategy of diimidazole spontaneous combustion materials. (a) Simple assembly of energy components of spontaneous combustion materials. (b) Structurally stable 1D chain HCPs were constructed from diimidazole.

To address the above challenges, we first proposed bridged bis-imidazole (bis(1-imidazolyl) methane = BIM) as a ligand to connect metal centers, thereby constructing reinforced frameworks and introducing highly active CBH anions *via* specific molecular design to build three isostructural HCPs $[M(CBH)_2(BIM)_2]_n$ (M = Cd **1**, Mn **2**, Zn **3**) (Scheme 1b). The neutral BIM ligand and the CBH anions were chosen for the following advantages: (i) unlike monodentate imidazole ligands that form isolated structures, bis-imidazole ligands feature two coordination sites capable of bridging coordination modes, thus potentially forming HCPs with structural reinforcement. (ii) In contrast to HAIM and HVIM ligands, which readily undergo deprotonation to form AIM^- and VIM^-, the BIM ligand remains neutral and has the capability to accommodate high-energy anions in HCPs. (iii) The CBH anions exhibit strong reducibility and high energy density, which can reduce ID time and improve the E_v values of HCPs.[30–32] As anticipated, the targeted HCPs were successfully synthesized, demonstrating potentially significant physical and energetic properties. The E_v values of **1–3** (E_v > 36.00 kJ cm^{-3}) are significantly higher than those of commercial UDMH (E_v = 25.60 kJ cm^{-3}),[20] as well as those reported for Cu-EIm-CBH (E_v = 33.47 kJ cm^{-3}),[26] Zn-VIm (Zn-VIm = $Zn(VIm)_2$, E_v = 18.90 kJ cm^{-3}), and Cd-VIm (Cd-VIm = $Cd(VIm)_2$, E_v = 15.80 kJ cm^{-3}).[25] Specifically, compounds **1–3** all demonstrate stable hypergolic performance, with ID times ranging from 12 to 27 ms. Notably, compound **2** exhibits the highest thermal stability (T_{dec} = 317 °C) among CBH-based hypergolic materials, attributed to its unique structural motif. Furthermore, the relationships between the structures and hypergolic properties are discussed both theoretically and experimentally.

Experimental section

Caution!

Metal nitrates, nitrogen-rich ligands, sodium cyanoborohydride, white fuming nitric acid (WFNA), and compounds **1–3** are all hazardous substances that may explode under friction, impact, and electrical discharge. All compounds should be used in small amounts, and appropriate protective measures should be taken during handling, including safety glasses, leather gloves, protective aprons, face masks, earplugs, and grounding devices.

Materials and instrumentation

All reagents and drugs were commercially obtained and used without further purification, and the ligand bis(1-imidazolyl) methane (BIM) was prepared following the literature method.[33] FT-IR spectra were determined using a PerkinElmer

This journal is © the Partner Organisations 2025

View Article Online

Published on 03 June 2025. Downloaded by Yunnan University on 7/31/2025 4:04:30 PM.

Spectrum using KBr disks ranging from 4000–400 cm^{-1}. Powder X-ray diffraction (PXRD) patterns were obtained using Cu Kα radiation (λ = 0.15406 nm) on a Rigaku Miniflex 600 diffractometer within the 2θ range of 5 to 50°. The simulated patterns were generated using Mercury Version 1.4 software. Elemental analysis (C, H, N) was performed using an Elementar Vario EL III microanalyzer. Thermogravimetric analysis (TGA) and differential scanning calorimetry (DSC) were conducted at a heating rate of 5 K min^{-1} under a N_2 atmosphere using a METTLER-TOLEDO instrument. The calorific value of combustion was determined using an oxygen bomb calorimeter (5E-AC8018, Changsha Kaiyuan Instrument Co., LTD, China). Impact sensitivity (IS) and friction sensitivity (FS) were analyzed using a BFH-12 BAM drop hammer and an FSKM-10 BAM tribometer, respectively. Ignition tests were recorded using the VEO710L high-speed camera from Vision Research Inc (AMETEKINC). FT-IR spectra are depicted in Fig. S1.† The experimental PXRD patterns are in good agreement with the simulated peaks, confirming the pure phase of **1–3** (Fig. S2†).

X-ray crystallography

A Rigaku FR-X microfocus diffractometer was used to obtain single crystal X-ray diffraction data using a Cu-Kα radiation source (λ = 1.54184 Å), T = 293 K, respectively. The crystal dataset is collected by ω-scanning technology, the structure of all non-hydrogen atoms is solved by direct methods, and the anisotropic thermal parameters on F^2 are corrected by the full matrix least squares method. The hydrogen atom is calculated at an ideal position, which allows dependence on its parent atom.[34,35] Tables S1 and S2† list the relevant crystal data, bond lengths, and bond angles for the compounds, respectively.

Ignition test

The ignition delay time is a crucial indicator for assessing whether a compound possesses self-ignition capabilities, defined as the interval between the initial contact of the oxidizer with the test sample and the appearance of sparks. The ID times for **1–3** were measured using "oxidizer-fuel" drop experiments and recorded using a high-speed camera capturing 5000 fps. Because the sensitivity of the samples is very low, it is a very insensitive energetic material. Therefore, the sample is dried at 75 °C for 2 h and fully ground for 30 min, using a 300-target test screen for screening treatment, and using an electronic balance to weigh 20 mg (error less than 1%) at the bottom of the glass bottle for testing.

Synthesis

The synthesis routes of **1–3** all employ diffusion methods as shown in Fig. 1 and the ESI.† Since the synthesis routes are similar, a detailed description of the synthesis process for **1** is provided as a representative example. Firstly, a solution of $Cd(NO_3)_2 \cdot 4H_2O$ (0.2 mmol, 61.69 mg) dissolved in water (5 mL) was prepared and placed at the bottom of the test tube. Subsequently, a mixture of acetonitrile and water (1 : 1, 5 mL) was slowly added onto the surface of the metal solution. Finally, a top layer of acetonitrile and water mixture (2 : 1, 6 mL) containing BIM (0.4 mmol, 59.20 mg) and $NaBH_3CN$ (0.4 mmol, 25.14 mg) were added. After 1 week, a substantial number of white crystals were obtained. Yield: 85% (based on BIM). Calcd for $C_{16}H_{24}N_{10}Cd$: C, 39.14; H, 4.89; N, 28.54%. Found: C, 39.97; H, 4.27; N, 28.11%. IR (KBr particle, cm^{-1}): 3110 s, 3024 w, 2340 vs, 2232 w, 2191 vs, 1711 w, 1604 w, 1507 s, 1391 s, 1285 s, 1236 vs, 1131 vs, 1086 vs, 1034 w, 932 m, 856 m, 755 s, 711 s, 658 s, 613 w (Fig. S1†).

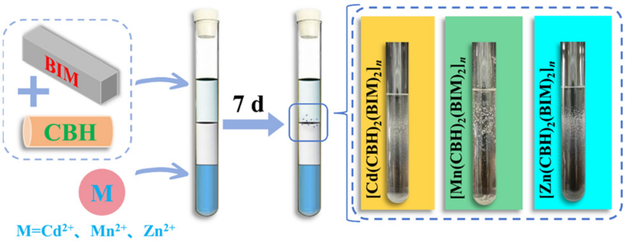

Fig. 1 Synthesis routes to **1–3**.

Results and discussion

Crystal structure

Single-crystal X-ray diffraction analysis reveals that **1** belongs to the orthorhombic crystal system, crystallizing in the space group *Cmce*, exhibiting a one-dimensional (1D) chain structure. The Cd(II) atom adopts a six-coordination pattern, forming an octahedral structure with six nitrogen atoms from four BIM ligands and two CBH^- anions (Fig. 2a). The axis of the octahedron is occupied by N11 and the symmetrically related N11#1, and the equatorial plane is occupied by N21, N21#1, N11#3, and N11#2. The Cd–N bond lengths are 2.33(3)

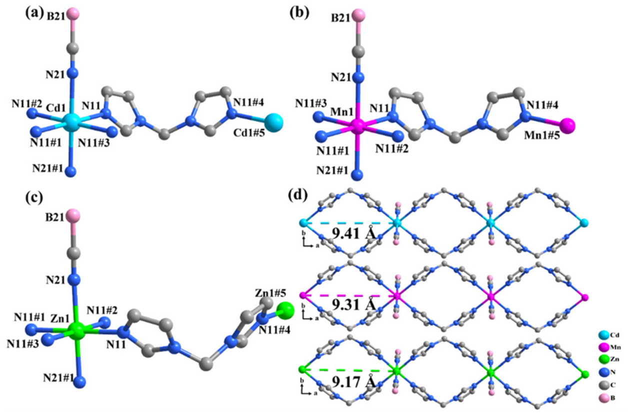

Fig. 2 Coordination environments of metal centers and ligands for **1** (a), **2** (b) and **3** (c); (d) the 1D chain diagrams for **1**, **2** and **3**. Symmetry codes for **1**, **2** and **3**. For **1**, #1 1 – *x*, 1 – *y*, 1 – *z*. #2 1 – *x*, *y*, *z*. #3 *x*, 1 – *y*, 1 – *z*. #4 2 – *x*, *y*, *z*. #5 1 + *x*, *y*, *z*. For **2**, #1 – *x*, 1 – *y*, 1 – *z*. #2 *x*, 1 – *y*, 1 – *z*. #3 – *x*, *y*, *z*. #4 1 – *x*, *y*, *z*. #5 1 + *x*, *y*, *z*. For **3**, #1 2 – *x*, 1 – *y*, 1 – *z*. #2 *x*, 1 – *y*, 1 – *z*. #3 2 – *x*, *y*, *z*. #4 1 – *x*, *y*, *z*. #5 – 1 + *x*, *y*, *z*.

Published on 03 June 2025. Downloaded by Yunnan University on 7/31/2025 4:04:30 PM.

Å (N21, N21#1) and 2.34(16) Å (N11, N11#1, N11#3, N11#2), respectively, and the N–Cd–N bond angles range from 86.14(8) to 180.0°. CBH$^-$ anions exhibit terminal coordination patterns. The BIM ligands with μ_2-κN11 : N11#4 coordination mode connect adjacent metal atom centers in the *c* direction in a to form an infinite zigzag 1D chain (Fig. 2d). The distance between two adjacent metal atoms (Cd⋯Cd) is 9.41 Å. These 1D chains extend in different directions and are further stacked through van der Waals force interactions to form 3D supramolecular structures (Fig. S3†).

Both **2** and **3** are isomorphic to **1**. In **2**, the distances of Mn–N are varying from 2.21(18) to 2.26(12) Å, and the bond angles of N–Mn–N are ranging from 86.41(6) to 180.0°, and the distance between neighboring Mn(II) centers is 9.31 Å in the 1D chain. In **3**, the Zn–N bond lengths fall in the range of 2.15 (2) to 2.17(14) Å, and the bond angles of N–Zn–N are between 86.74(8) to 180.0°, The distance between two adjacent metal atoms (Zn⋯Zn) in the 1D chain is 9.17 Å. Their detailed structures are shown in Fig. 2 and Fig. S3.† The PLATON software calculation results show that the total void volumes of **1–3** are all approximately zero. These results indicate that **1–3** hold a relatively tightly packed structure with the densities (ρ) of **1–3** between 1.32 to 1.47 g cm^{-3}. Compared with the reported ZIF-based Cd-VIm (ρ = 0.98 g cm^{-3}), Zn-VIm (ρ = 0.99 g cm^{-3}),[25] and other CBH-based HCCs with ρ between 1.18 to 1.30 g cm^{-3} (Table S4†),[26,36] the densities of CBH-based **1–3** are significantly enhanced through the structural design strategy.

Physicochemical properties

The thermal stabilities of **1–3** were evaluated by thermogravimetric analysis (TGA) and differential scanning calorimetry (DSC). The experimental results showed that **1–3** experienced rapid weight loss at 268, 317 and 248 °C, respectively (Fig. 3). These results agree well with the distinct exothermic peaks observed at 280, 322, and 264 °C in the DSC curves of **1–3**. Compounds **1–3** exhibit remarkable thermal stability compared to most reported HCCs (Table 1). To the best of our knowledge, Mn-based **2** has the highest decomposition temperature among CBH$^-$-based hypergolic materials (Fig. 4). The high thermal stability can be attributed to the unique tightly packed structures resulting from the coordination polymerization of CBH$^-$ anions and bis-imidazole ligands.

To further evaluate the stabilities of **1–3** in different environments, compounds **1–3** were placed in water (7 days) and at 75 °C (8 hours), respectively. The experimental PXRD results indicate that **1–3** maintain excellent chemical stability after being exposed to water for one week or to 75 °C for 8 hours (Fig. 5). Mechanical sensitivity is an important indicator for evaluating the safety of energetic materials (for

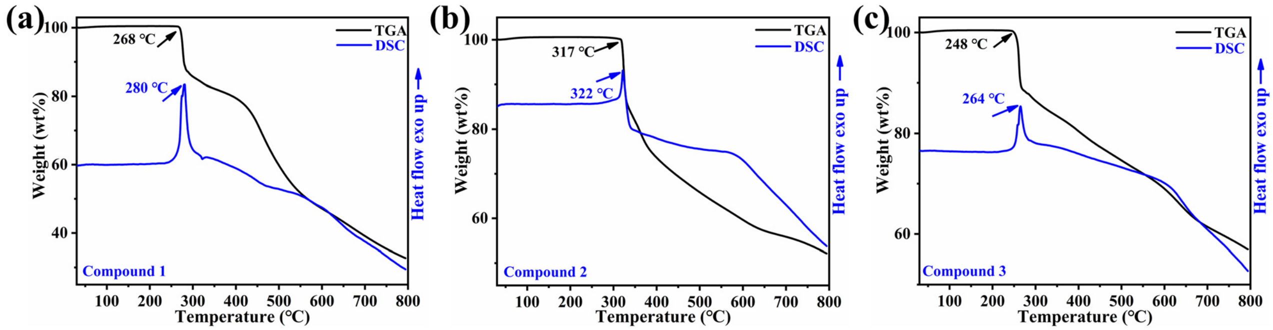

Fig. 3 DSC and TGA curves of **1** (a), **2** (b) and **3** (c).

Table 1 Physicochemical properties of **1–3** and other reported hypergolic materials

Compound	ρ [a] g cm^{-1}	T_{dec} [b] °C	IS [c] (J)	FS [d] (N)	E_g [e] kJ g^{-1}	E_v [f] kJ cm^{-3}	I_{sp} [g] s	ID [h] ms
1	1.47	268	>40	>360	37.53	25.52	223	12
2	1.32	317	>40	>360	37.99	28.59	225	13
3	1.40	248	>40	>360	36.73	26.22	219	27
Cu-MIm-CBH[26]	1.30	182	>40	>360	35.03	26.95	223	9
Cu-EIm-CBH[26]	1.20	193	>40	>360	33.47	27.87	230	10
Cu-AIm-CBH[26]	1.25	178	>40	>360	36.67	29.27	226	4
Cu-VIm-CBH[26]	1.28	163	>40	>360	34.68	27.03	222	2
Mn-AIm-CBH[36]	1.18	248	—	—	—	—	271	24
Ni-AIm-CBH[36]	1.22	165	—	—	—	—	269	25
Zn-VIm[25]	0.99	>250	—	—	18.90	19.00	—	29
Cd-VIm[25]	0.98	>250	—	—	15.80	16.10	—	35
UDMH[20]	0.78	62	—	—	25.60	33.10	239	4.8

[a] Density. [b] Thermal stability. [c] Impact sensitivity. [d] Friction sensitivity. [e] Volumetric energy densities. [f] Gravimetric energy densities. [g] Specific impulse. [h] Ignition delay time.

Published on 03 June 2025. Downloaded by Yunnan University on 7/31/2025 4:04:30 PM.

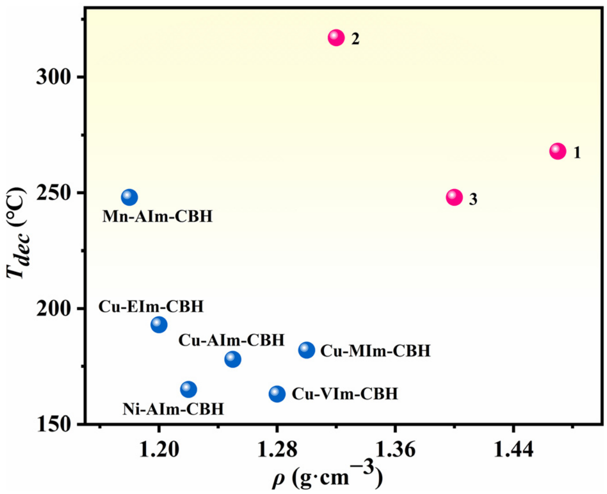

Fig. 4 Comparison of the decomposition temperatures and densities of HCPs with those of other published CBH-based fuels.

experimental details see the ESI†). The IS values of **1–3** are all greater than 40 J, as determined by the standard BAM drop hammer test, and the FS values are greater than 360 N, as determined by the standard BAM friction test techniques. According to the "United Nations Recommendations on the Transport of Dangerous Goods",[37] compounds **1–3** are classified as insensitive energetic materials, meeting the safety requirements for the use and transportation of propellants. These results demonstrate that these compounds may be suitable for use under harsh conditions.

The enthalpy of combustion ($\Delta_c H$) of the compounds was determined and calculated using the oxygen bomb calorimetry method, with experimental $\Delta_c H$ values of **1–3** being −12 515.24, −12 379.68, and −11 624.88 kJ mol^{-1}, respectively (see the ESI†). The mass energy density (E_g) and E_v of **1–3** are derived from the $\Delta_c H$ values. The E_g values of **1–3** are 25.52, 28.59 and 26.22 kJ g^{-1}, respectively, and the E_v values of **1–3** are 37.53, 37.99 and 36.73 kJ cm^{-3}, respectively. The E_v values of **1–3** are not only higher than those of Zn-VIm (E_v = 18.90 kJ cm^{-3}),[25] Cd-VIm (E_v = 15.80 kJ cm^{-3})[25] and Cu-VIm-CBH (E_v = 34.68 kJ cm^{-3}),[26] but also higher than that of the commercial UDMH (E_v = 25.60 kJ cm^{-3}),[20] which can be attributed to the high densities of **1–3**.

The standard enthalpy of formation ($\Delta_f H°$) values of **1–3** are calculated from the Hess thermochemical cycle reaction and are 1258.78, 996.72 and 276.32 kJ mol^{-1}, respectively (see the ESI†). The specific impulse of the compound was calculated using the chemical equilibrium application (CEA) developed by NASA researchers.[9,38,39] The selection of specific parameters is given in the ESI. The results showed that compounds **1–3** exhibited the largest I_{sp} values at O/F = 2, which were 223 s, 225 s and 219 s, respectively. The I_{sp} values of **1–3** are comparable to that of UDMH (I_{sp} = 239 s),[20] suggesting that these compounds have the potential to be used as high-performance propellant fuels.

Ignition properties

WFNA was used as the oxidizer to evaluate the spontaneous combustion characteristics of **1** to **3** using the "oxidizer-dropping" experiment. The ignition delay time is defined as the interval from the moment the oxidizer contacts the fuel until the appearance of the first flame.[1] The entire combustion process was captured using a high-speed camera. The complete reaction processes of **1–3** are shown in Fig. 6. Under the same conditions, the combustion behavior of BIM ligands and the oxidizer was also tested. The results indicate that **1–3** ignited and emitted bright yellow flames, with ID values of 12, 13, and 27 ms respectively, whereas the BIM ligands did not self-ignite. At an equal mass of 20 mg, compound **1** produced the highest flame, exceeding 10 cm in height. The flame heights of **2** and **3** were approximately 8 cm and 7 cm, respectively, indicating that **1** is capable of releasing a greater amount of energy. All three compounds exhibit a shorter ignition delay time and stable combustion characteristics, with combustion behavior more competitive than that of Zn-VIM (ID = 29 ms) and Cd-VIm (ID = 35 ms).[25] Notably, compounds **1–3** share similar structural characteristics, suggesting that metal ion centers play a significant role in spontaneous ignition behavior.

Discussion on relationships between structure and properties

To thoroughly investigate the intermolecular interactions in **1–3**, the Hirshfeld surfaces and 2D fingerprint plots were cal-

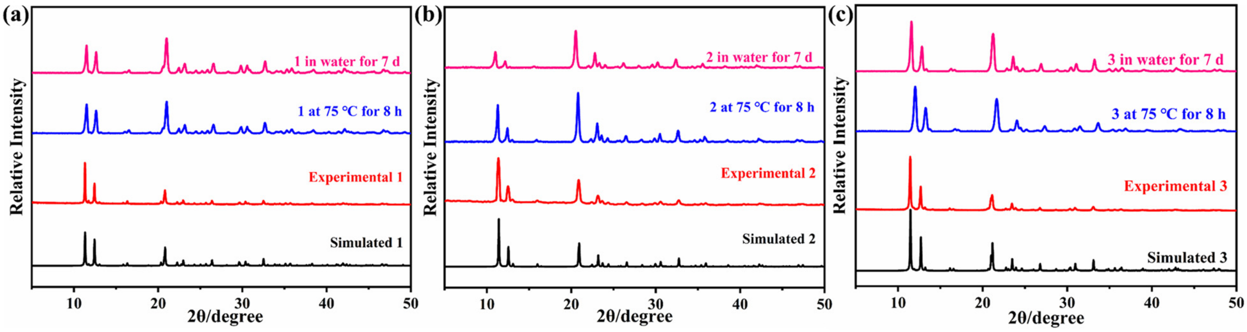

Fig. 5 PXRD comparison of **1** (a), **2** (b) and **3** (c) under different conditions.

Published on 03 June 2025. Downloaded by Yunnan University on 7/31/2025 4:04:30 PM.

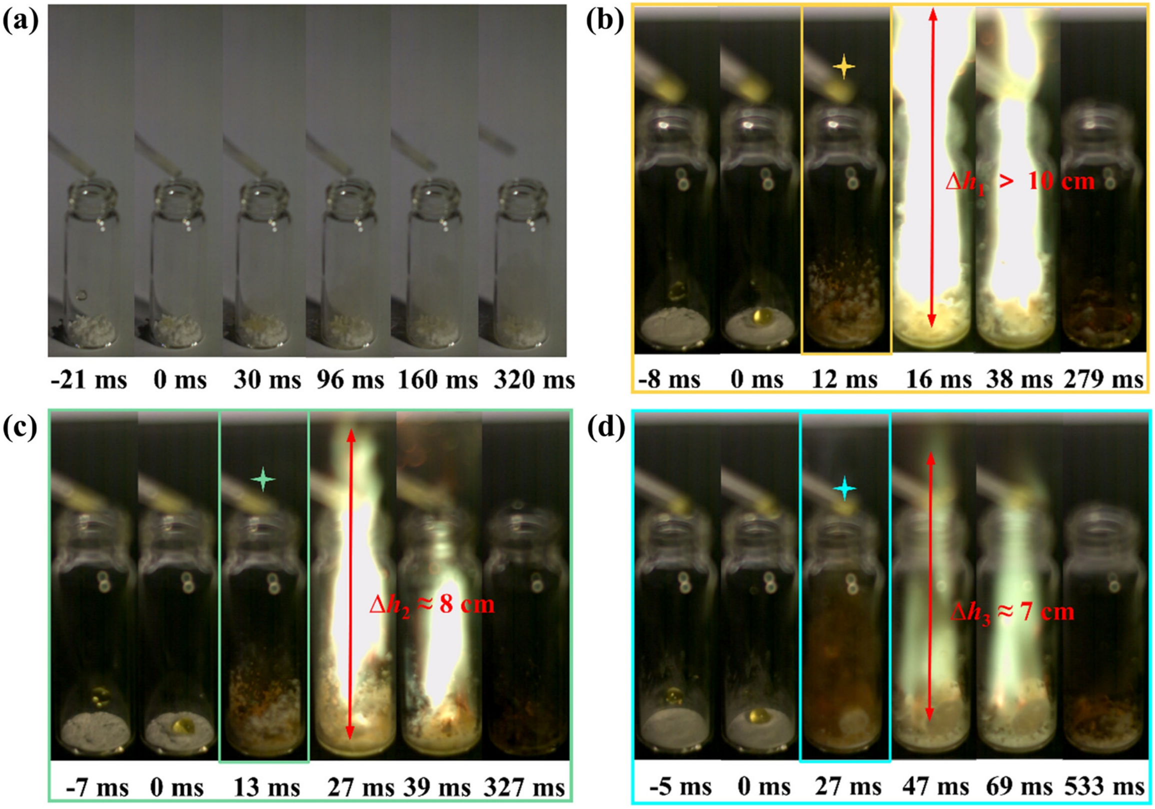

Fig. 6 Reaction process between the BIM ligand (a), **1** (b), **2** (c) and **3** (d) and oxidizer WFNA under a high-speed camera. The asterisk indicates the first fire.

culated using Crystal Explorer 21.5 software, and pie charts of the corresponding data distributions were generated (Fig. 7a–c).[40,41] The results show that all compounds appear red spots at the metal atoms, indicating strong inter-molecular interactions such as Cd⋯N/N⋯Cd, Mn⋯N/N⋯Mn, and Zn⋯N/N⋯Zn. Additionally, large areas of blue and white spots on the Hirshfeld surfaces indicate the presence of weak interactions among N⋯N, N⋯C, N⋯B, *etc*. The data distribution diagrams reveal that in **1** and **2**, H⋯B/B⋯H and H⋯N/N⋯H interactions constitute over 37% of the hydrogen bonding network, while in **3**, these interactions comprise 19.70%. The presence of hydrogen bonds positively affects stability, which is consistent with **1** and **2** exhibiting higher thermal decomposition temperatures.

To analyze the role of CBH^- anions and metal ions in spontaneous combustion properties, we performed density functional theory (DFT) calculations on **1**–**3** and conducted an electrostatic potential (ESP) study (Fig. 7d–f).[19,42] The calculations indicate that the CBH^- anion in **1**–**3** exhibits strong nucleophilicity suggesting a higher likelihood of reacting with HNO_3. Notably, the Cd^{2+} in **1** exhibits a stronger polarization effect compared to **2** and **3**, suggesting higher reactivity, consistent with its shortest ignition delay time.[43] Based on these computational results, we hypothesize that metal atoms may play a catalytic role during the autoignition process, potentially reducing the ignition delay time.

To further investigate the relationship between structure and autoignition behavior, we employed molecular orbital theory to explain the chemical behaviors. For compounds with similar components and structures, the energy gap ($\Delta E_{\text{L–H}}$) between the highest occupied molecular orbital (HOMO) and the lowest unoccupied molecular orbital (LUMO) partially reflects each of their kinetic stability and reactivity in chemical reactions.[7,44] Generally, a smaller energy gap indicates higher reactivity and a greater propensity to react with oxidizers.[45–48] To this end, we used Materials Studio 2019 software to calculate the molecular orbitals of **1**–**3** and determined their energy gap values (Fig. 7g–l).[9] The results indicate that **1** and **3** have similar HOMO distributions, primarily concentrated around the CBH^- anions. The HOMO frontier orbitals of **2** are primarily distributed around the metal atom and the coordinating nitrogen atoms of the BIM ligand. The LUMO distribution patterns for **1**–**3** are similar, confined to the CBH^- anions and the coordinating nitrogen atoms. The calculated $\Delta E_{\text{L–H}}$ values for **1**–**3** are 0.04, 0.05, and 0.07 eV, respectively. The drop test results show ID(**1**) < ID(**2**) < ID(**3**), consistent with the computed results. The three compounds have similar structural features, but **1** exhibits a relatively smaller energy gap, which we speculate may be due to the metal atoms partially adjusting their molecular orbital distribution. This result is consistent with the density of states calculations (Fig. S5†).[49,50] Based on this analysis, we conclude that metal ions play a crucial regulatory role in autoignition behaviors.

This journal is © the Partner Organisations 2025

Published on 03 June 2025. Downloaded by Yunnan University on 7/31/2025 4:04:30 PM.

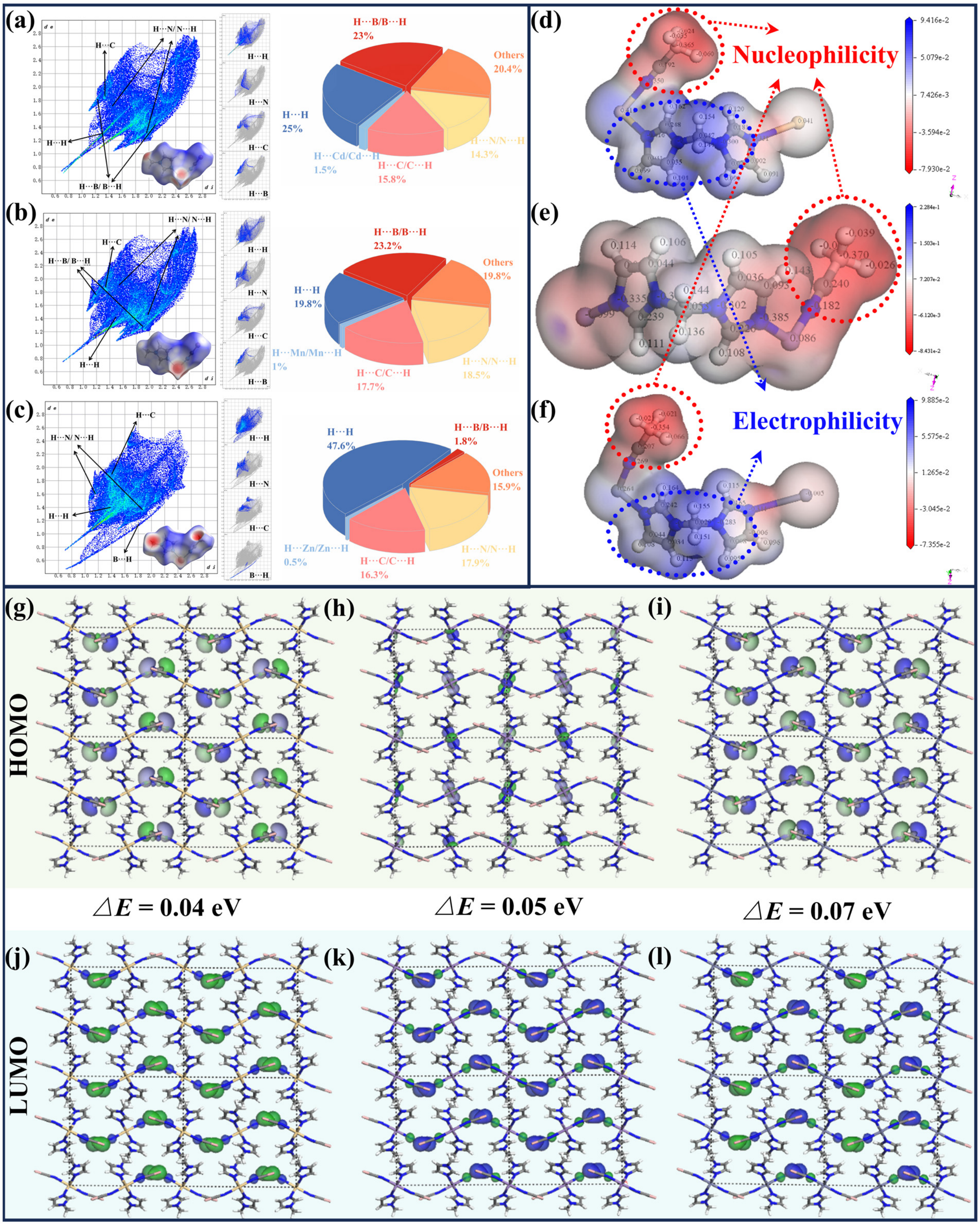

Fig. 7 Hirshfeld surface and molecular interaction distribution population of **1** (a), **2** (b), and **3** (c); the ESP mapping of **1** (d), **2** (e), and **3** (f); the HOMO molecular orbital distribution of **1** (g), **2** (h), and **3** (i); the LUMO molecular orbital distribution of **1** (j), **2** (k), and **3** (l).

Conclusions

In summary, we first introduced CBH^- anions into coordination polymers by selecting neutral and bridged bis-imidazole linkers, synthesizing three isomeric and hypergolic CPs. All three compounds exhibit hypergolic properties and maintain good structural stabilities under various conditions. To the best of our knowledge, compound **2** exhibits the highest

Published on 03 June 2025. Downloaded by Yunnan University on 7/31/2025 4:04:30 PM.

thermal stabilities among all CBH$^-$-based hypergolic materials. Furthermore, these compounds also display remarkable energy densities (36.73–37.99 kJ cm^{-3}), significantly exceeding that of commercial UDMH (E_v = 25.60 kJ cm^{-3}).[19] The Cd-based **1** undergoes spontaneous ignition upon reaction with the oxidizer WFNA, exhibiting the shortest ignition delay time of 12 ms. Theoretical calculations analyzed the relationships between structures and spontaneous ignition performances, suggesting that the varying ID times among these compounds may be attributed to the differing extents of modulation by the metal ion centers and CBH$^-$ anions in their ignition behavior. This study provides a new insight into the preparation of next-generation high-energy, safe hypergolic materials through a precise structural design strategy.

Author contributions

Qin Wang designed, synthesized the compounds, and drafted the manuscript. Meng Cui was instrumental in conceiving the experiments, analyzing and discussing the results and revising the manuscript. Pin-Hao Wei, Long-Chuan Li, and Ning-Ning Zhang assisted in the experiment. Fei Tan revised the manuscript. Jian-Gang Xu contributed to the crystal structure analysis, interpretation of experimental outcomes, and revised the manuscript. Guo-Cong Guo and Fa-Kun Zheng conceived the experiments and revised the manuscript. All authors have reviewed and approved the final manuscript.

Data availability

The data supporting this article have been included as part of the ESI.†

Conflicts of interest

The authors declare that they have no known competing financial interests or personal relationships that could have appeared to influence the work reported in this paper.

Acknowledgements

The authors acknowledge financial support from the National Natural Science Foundation of China (22201037), and the Natural Science Foundation of Fujian Province (2021J01106).

References

1 Q. H. Zhang and J. M. Shreeve, Energetic Ionic Liquids as Explosives and Propellant Fuels: A New Journey of Ionic Liquid Chemistry, *Chem. Rev.*, 2014, **114**, 10527–10574.

2 H. H. Gao, Y. H. Joo, B. Twamley, Z. Q. Zhou and J. M. Shreeve, Hypergolic Ionic Liquids with the 2,2-Dialkyltriazanium Cationm, *Angew. Chem., Int. Ed.*, 2009, **48**, 2792–2795.

3 H. M. Titi, M. Arhangelskis, G. P. Rachiero, T. Friščić and R. D. Rogers, Hypergolic Triggers as Cocrystal Formers: Cocrystallization for Creating New Hypergolic Materials with Tunable Energy Content, *Angew. Chem.*, 2019, **131**, 18570–18575.

4 Q. Y. Wang, J. Wang, S. Wang, Z. Y. Wang, M. Cao, C. L. He, J. Q. Yang, S. Q. Zang and T. C. W. Mak, o-Carborane-Based and Atomically Precise Metal Clusters as Hypergolic Materials, *J. Am. Chem. Soc.*, 2020, **142**, 12010–12014.

5 M. J. Baier, P. V. Ramachandran and S. F. Son, Characterization of the Hypergolic Ignition Delay of Ammonia Borane, *J. Propul. Power*, 2019, **35**, 182–189.

6 B. S. Wang, Z. Wang, Y. H. Jin and K. C. Wang, Designing Difunctional Promoters for Hypergolic Ignitions of Green Bipropellants Combining Ionic Liquids with H_2O_2, *Ind. Eng. Chem. Res.*, 2022, **61**, 17433–17439.

7 W. L. Yuan, L. Zhang, G. H. Tao, S. L. Wang, Y. Wang, Q. H. Zhu, G. H. Zhang, Z. Zhang, Y. Xue, S. Qin, L. He and J. M. Shreeve, Designing high-performance hypergolic propellants based on materials genome, *Sci. Adv.*, 2020, **6**, eabb1899.

8 L. H. Fei, M. X. Qin, Z. H. Huang and C. L. Tang, Different Ignition Modes and Temperature Evolution of Typical Hypergolic Ionic Liquids, *Energy Fuels*, 2023, **37**, 7372–7379.

9 H. Y. Bian, Y. F. Yan, M. Cui, T. T. Song, X. D. Guo, J. G. Xu, F. K. Zheng and G. C. Guo, Energetic isostructural metal imidazolate frameworks with a bridging dicyanamide linker towards high-performance hypergolic fuels, *Inorg. Chem. Front.*, 2023, **10**, 5468–5474.

10 T. M. Klapötke, N. K. Minar and J. Stierstorfer, Investigations of bis(methyltetrazolyl)triazenes as nitrogen-rich ingredients in solid rocket propellants-Synthesis, characterization and properties, *Polyhedron*, 2009, **28**, 13–26.

11 S. W. Song, Y. Wang, W. He, K. C. Wang, M. Yan, Q. L. Yan and Q. H. Zhang, Melamine N-oxide based self-assembled energetic materials with balanced energy & sensitivity and enhanced combustion behavior, *Chem. Eng. J.*, 2020, **395**, 125114.

12 C. Wang, C. Li, Z. Duan, Z. F. Wang, Q. Y. Wang and S. Q. Zang, Engineering High-Performance Hypergolic Propellant by Synergistic Contribution of Metal–Organic Framework Shell and Aluminum Core, *Small*, 2024, **20**, 2310970.

13 Y. Q. Zhang, H. X. Gao, Y. H. Joo and J. M. Shreeve, Ionic Liquids as Hypergolic Fuels, *Angew. Chem., Int. Ed.*, 2011, **50**, 9554–9562.

14 Y. Zhang and J. M. Shreeve, Dicyanoborate-Based Ionic Liquids as Hypergolic Fluids, *Angew. Chem., Int. Ed.*, 2011, **50**, 935–937.

15 Q. H. Zhang and J. M. Shreeve, Ionic Liquid Propellants: Future Fuels for Space Propulsion, *Chem. – Eur. J.*, 2013, **19**, 15446–15451.

Published on 03 June 2025. Downloaded by Yunnan University on 7/31/2025 4:04:30 PM.

16 Q. H. Zhang, P. Yin, J. H. Zhang and J. M. Shreeve, Cyanoborohydride-Based Ionic Liquids as Green Aerospace Bipropellant Fuels, *Chem. – Eur. J.*, 2014, **20**, 1–7.

17 S. D. Chambreau, S. Schneider, M. Rosander, T. Hawkins, C. J. Gallegos, M. F. Pastewait and G. L. Vaghjiani, Fourier Transform Infrared Studies in Hypergolic Ignition of Ionic Liquids, *J. Phys. Chem. A*, 2008, **112**, 7816–7824.

18 W. J. Zhou, J. B. Liu, S. D. Chambreau and G. L. Vaghjiani, Molecular Dynamics Simulations, Reaction Pathway and Mechanism Dissection, and Kinetics Modeling of the Nitric Acid Oxidation of Dicyanamide and Dicyanoborohydride Anions, *J. Phys. Chem. B*, 2020, **124**, 11175–11188.

19 Y. H. Jin, Y. T. Shi, X. J. Qi, S. Huang and Q. H. Zhang, Theoretical Study on Hydrolytic Stability of Borohydride-Rich Hypergolic Ionic Liquids, *J. Phys. Chem. A*, 2020, **124.**, 2942–2950.

20 Z. M. Li, Y. Q. Xu, C. Wang, G. R. Lei, R. Zhang, L. Zhang, J. H. Chen, J. G. Zhang, T. L. Zhang and Q. Y. Wang, "All-in-one" hypergolic metal-organic frameworks with high energy density and short ignition delay, *J. Mater. Chem. A*, 2022, **10**, 2795–2799.

21 C. Shen, Y. G. Xu and M. Lu, A series of high-energy coordination polymers with 3,6-bis(4nitroamino-1,2,5-oxadiazol-3-yl)-1,4,2,5-dioxadiazine, a ligand with multi-coordination sites, high oxygen content and detonation performance: Syntheses, structures, and performance, *J. Mater. Chem. A*, 2012, 1–3.

22 Y. Q. Xu, Y. N. Wang, Y. Zhong, G. R. Lei, Z. M. Li, J. G. Zhang and T. L. Zhang, High-Energy Metal-Organic Frameworks with a Dicyanamide Linker for Hypergolic Fuels, *Inorg. Chem.*, 2021, **60**, 5100–5106.

23 H. F. Wu, J. G. Xu, J. Lu, F. K. Zheng, S. H. Wang and G. C. Guo, Highly Stable Energetic Coordination Polymer Assembled with Co(II) and Tetrazole Derivatives, *ACS Omega*, 2019, **4**, 15107–15111.

24 T. W. Wang, Z. X. Yi, L. Zhang, Y. K. Wang, Y. Li and J. G. Zhang, Top Development of Green-Light Pyrotechnics: Hypergolic Cu(II) Based Coordination Polymers, *Cryst. Growth Des.*, 2023, **23**, 558–564.

25 H. M. Titi, J. M. Marrett, G. Dayaker, M. Arhangelskis, C. Mottillo, A. J. Morris, G. P. Rachiero, T. Friščić and R. D. Rogers, Hypergolic zeolitic imidazolate frameworks (ZIFs) as next-generation solid fuels: Unlocking the latent energetic behavior of ZIFs, *Sci. Adv.*, 2019, **5**, eaav9044.

26 L. N. Liang, Y. Zhong, Y. Q. Xu, G. R. Lei, J. M. Chen, H. S. Huang, Z. M. Li, J. G. Zhang and T. L. Zhang, Cyanoborohydride (CBH)-based hypergolic coordination compounds for versatile fuels, *Chem. Eng. J.*, 2021, **426**, 131866.

27 Y. J. Wang, X. Y. Wang, H. Xu, W. W. Ren, R. Pang, L. Yang, W. C. Tong, Q. Y. Wang and S. Q. Zang, One-dimensional copper bromide based inorganic-organic hybrids as fuels for hypergolic bipropellants with hydrogen peroxide as oxidizer, *Chem. Eng. J.*, 2023, **455**, 140587.

28 K. C. Wang, Z. Wang, X. Zhao, X. J. Qi, S. W. Song, Y. H. Jin and Q. H. Zhang, Unearthing hidden hypergolic potential of energetic complexes with hydrogen peroxide, *Combust. Flame*, 2022, **244**, 112235.

29 J. Das, D. Shem-Tov, S. Z. Wang, L. Zhang, E. Flaxer, S. J. Zhang, J. Stierstorfer, K. C. Wang, Q. L. Yan, R. Dobrovetsky and M. Gozin, Hydride-and boron-free solid hypergolic H_2O_2-ignitophores, *Chem. Eng. J.*, 2021, **426**, 131806.

30 Z. J. Zhang, Y. Q. Zhang, Z. M. Li, N. M. Jiao, L. Liu and S. J. Zhang, $B_{12}H_{12}^{2-}$-Based Metal (Cu^{2+}, Ni^{2+}, Zn^{2+}) Complexes as Hypergolic Fuels with Superior Hypergolicity, *Eur. J. Inorg. Chem.*, 2018, **8**, 981–986.

31 V. K. Bhosale and P. S. Kulkarni, Hypergolic Behavior of Pyridinium Salts Containing Cyanoborohydride and Dicyanamide Anions with Oxidizer RFNA, *Propellants, Explos., Pyrotech.*, 2016, **41**, 1013–1019.

32 C. G. Sun, S. K. Tang and X. W. Zhang, Hypergolicity evaluation and prediction of ionic liquids based on hypergolic reactive groups, *Combust. Flame*, 2019, **205**, 441–445.

33 Z. X. Fu, J. Lin, L. Wang, C. Li, W. B. Yan and T. Wu, Cuprous Iodide Pseudo-Polymorphs Based on Imidazole Ligand and Their Luminescence Thermochromism, *Cryst. Growth Des.*, 2016, **16**, 2322–2327.

34 G. M. Sheldrick, SHELXT-Integrated space-group and crystal structure determination, *Acta Crystallogr.*, 2015, **71**, 3–8.

35 L. J. Bourhis, O. V. Dolomanov, R. J. Gildea, J. A. K. Howard and H. Puschmann, The anatomy of a comprehensive constrained, restrained refinement program for the modern computing environment-Olex2 dissected, *Acta Crystallogr.*, 2015, **71**, 59–75.

36 X. Zhao, Z. Wang, X. J. Qi, S. W. Song, S. Huang, K. C. Wang and Q. H. Zhang, Hunting for Energetic Complexes as Hypergolic Promoters for Green Propellants Using Hydrogen Peroxide as Oxidizer, *Inorg. Chem.*, 2021, **60**, 17033–17039.

37 Impact: insensitive > 40 J, less sensitive ≥ 35 J, sensitive ≥ 4 J, very sensitive ≤ 3 J; friction: insensitive > 360 N, less sensitive = 360 N, 80 N < sensitive < 360 N, very sensitive ≤ 80 N, extremely sensitive ≤ 10 N.

38 R. Sunil, A. Virkar, M. V. Kumar, I. Krishnamoorthy and V. Malhotra, Combustion and propulsive characteristics of potential hybrid rocket propellant, *IOP Conf. Ser.: Mater. Sci. Eng.*, 2020, **912**, 042023.

39 Z. Y. Zhang, Z. R. Zhao, B. S. Wang and J. H. Zhang, Boron based hypergolic ionic liquids: A review, *Green Energy Environ.*, 2021, **6**, 794–822.

40 S. J. Li, R. P. Bu, R. J. Gou and C. Y. Zhang, Hirshfeld Surface Method and Its Application in Energetic Crystals, *Cryst. Growth Des.*, 2021, **21**, 6619–6634.

41 M. A. Spackman and D. Jayatilaka, Hirshfeld surface analysis, *CrystEngComm*, 2009, **11**, 19–32.

42 T. W. Wang, Z. X. Yi, X. J. Wang, W. L. Cao, S. G. Zhu and J. G. Zhang, Preparation of Laser Energetic Coordination Polymers Based on Urazine by Self-Crystallization, *ACS Appl. Mater. Interfaces*, 2022, **14**, 16718–16726.

Published on 03 June 2025. Downloaded by Yunnan University on 7/31/2025 4:04:30 PM.

43 T. L. Pu, X. Y. Wang, Z. Duan, Z. B. Sun, X. Y. Dong, Q. Y. Wang, S. Q. Zang, J. H. Huang, A. Q. Ji, Z. Duan, Z. Y. Wang, Q. Y. Wang and S. Q. Zang, Boosting 2000-Fold Hypergolic Ignition Rate of Carborane by Substitutes Migration in Metal Clusters, *Angew. Chem., Int. Ed.*, 2024, **63**, e202402363.

44 Z. X. Zhou and R. G. Parr, Activation Hardness: New Index for Describing the Orientation of Electrophilic Aromatic Substitution, *J. Am. Chem. Soc.*, 1990, **112**, 5720–5724.

45 S. Q. Li, H. X. Gao and J. M. Shreeve, Borohydride Ionic Liquids and Borane/Ionic-Liquid Solutions as Hypergolic Fuels with Superior Low Ignition-Delay Times, *Angew. Chem.*, 2014, **126**, 3013–3016.

46 L. M. Qiu, D. Y. Ye, W. Wei, K. H. Chen, J. X. Hou, J. Zheng, X. D. Gong and H. M. Xiao, DFT studies toward the design and properties of high-energy density hydrocarbon fuel, *J. Mol. Struct.: THEOCHEM*, 2008, **866**, 63–74.

47 J. I. Aihara, Reduced HOMO-LUMO Gap as an Index of Kinetic Stability for Polycyclic Aromatic Hydrocarbons, *J. Phys. Chem. A*, 1999, **103**, 7487–7495.

48 J. H. Huang, A. Q. Ji, Z. Duan, Z. Y. Wang, Q. Y. Wang and S. Q. Zang, Boosting 2000-Fold Hypergolic Ignition Rate of Carborane by Substitutes Migration in Metal Clusters, *Adv. Sci.*, 2024, **11**, 2401861.

49 P. K. Wang, W. F. Wang, B. Y. Li, M. J. Xie, H. Y. Bian, S. H. Wang, F. K. Zheng and G. C. Guo, Flexible strontium-based metal-organic framework scintillation screens for high-resolution X-ray imaging, *Inorg. Chem. Front.*, 2023, **10**, 5710–5718.

50 M. Cui, Y. F. Yan, R. X. Qian, B. W. Fan, H. Y. Bian, F. Wen, J. G. Xu, F. K. Zheng and G. C. Guo, Structure-Induced Energetic Coordination Compounds as Additives for Laser Initiation Primary Explosives, *Adv. Mater.*, 2024, 2414886.

51 Q. Wang, CCDC 2329585: *CSD Communication*, 2025, DOI: 10.5517/ccdc.csd.cc2j63xs.

This journal is © the Partner Organisations 2025